Observation of Velocity-Independent Electron Transport in the Reversed Field Pinch

R. O'Connell,* D. J. Den Hartog, C. B. Forest, J. K. Anderson, T. M. Biewer,† B. E. Chapman, D. Craig, G. Fiksel, S. C. Prager, J. S. Sarff, and S. D. Terry‡

Department of Physics, University of Wisconsin–Madison, Madison, Wisconsin 53706, USA

R.W. Harvey

CompX, San Diego, California, USA

(Received 16 December 2002; published 24 July 2003)

Confinement of runaway electrons has been observed for the first time in a reversed field pinch during improved-confinement plasmas in the Madison Symmetric Torus. Energy-resolved hard-x-ray flux measurements have been used to determine the velocity dependence of the electron diffusion coefficient, utilizing computational solutions of the Fokker-Planck transport equation. With improved-confinement, the fast electron diffusivity drops by 2 orders of magnitude and is independent of velocity. This suggests a change in the transport mechanism away from stochastic magnetic field diffusion.

DOI: 10.1103/PhysRevLett.91.045002 PACS numbers: 52.55.Hc, 52.25.Fi, 52.70.La

Energy loss in magnetically confined toroidal plasmas for thermonuclear fusion research is dominated by fluctuation driven transport [1]. In the standard reversed field pinch (RFP) configuration, transport in the core of the plasma is believed to arise from fluctuations in the magnetic field. Multiple, overlapping, unstable resistive tearing modes cause field lines to reconnect, generating a small radial component to the magnetic field which leads to field lines that wander stochastically, slowly diffusing across the plasma. Flow along the field lines is expected to cause rapid particle and energy loss [2].

Recently, energy loss in RFP experiments has been reduced tenfold through modification of the current density profile, the source of the free energy for the tearing instabilities [3,4]. It has been conjectured that the improved confinement of the bulk plasma energy results from reduction of the magnetic stochasticity. However, stochasticity of magnetic field line trajectories is not directly measurable. A common simple estimate of the diffusion coefficient is $D_{RR} = v_{||}D_M$, where D_{RR} is the Rechester-Rosenbluth model for the electron particle radial diffusion coefficient, $v_{||}$ is the parallel electron velocity, $D_M = (\langle \Delta r^2 \rangle / 2\Delta l)$ is the diffusion coefficient of the magnetic field lines, and Δr is the radial displacement from equilibrium after tracing a length Δl along a field line [5]. The faster the electron, the more rapidly it streams along the field line and is lost from the plasma. Hence the behavior of fast electrons is a particularly sensitive indicator of magnetic stochasticity.

In this Letter, we compare measurements of D_r in standard plasmas (which have poor energy confinement and large-amplitude magnetic fluctuations) and improved-confinement plasmas (in which there is an order of magnitude increase in energy confinement and the magnetic fluctuations are reduced). The fast electrons are detected by hard-x-ray (HXR) emission from electron-ion bremsstrahlung. The velocity dependence of the electron diffusion is obtained through solution of the electron Fokker-Planck equation, using the HXR measurements as input. X-ray measurements taken during standard plasmas are consistent with previous observations of emission from runaway electrons in the RFP, with typical peak energies up to ~10 keV [6–8]. During standard plasmas there is a dearth of electrons above 10 keV and the computed D_r is found to be proportional to electron speed, which is consistent with magnetic stochastic diffusion.

In contrast, during improved-confinement plasmas, electrons with energy up to 100 keV are observed and well confined. Their diffusion is reduced, relative to standard plasmas, by 2 orders of magnitude, and D_r is roughly independent of velocity. These results are inconsistent with the theoretical expectation for transport from magnetic stochasticity. This suggests that such RFP plasmas have transitioned to a new regime no longer dominated by magnetic stochasticity.

The experiments reported here were performed in the Madison Symmetric Torus (MST), a reversed field pinch with a 1.5 m major radius and 0.52 m minor radius [9]. The plasma is driven inductively, with plasma currents up to 500 kA. Typical core plasma densities are 1×10^{19} m^{-3}. The core electron temperature varies from ~0.2–0.5 keV for standard plasmas to ~0.6–1.3 keV for improved-confinement plasmas. The energy confinement time extends up to 10 ms [3,4].

The hard-x-ray flux is measured with solid state cadmium-zinc-telluride (CdZnTe) detectors. Two lines of sight are used: one views along a minor radius through the plasma core, the other views the plasma edge ($r/a > 0.8$). During the improved-confinement phase the flux from the core line of sight is ≈ 100 times higher than that from the edge, showing that the emission is concentrated in the plasma core. The detectors are sensitive to photons from ~10 to 300 keV [10], which for these plasma conditions is dominated by bremsstrahlung since it is above the energy for known line emission. X-ray events are digitized directly, providing superb noise and pileup immunity with zero dead time. Energy resolution is limited only by the detector resolution ($\sim 10\%$ of photon energy). Count rates up to 500 kHz can be resolved, with submicrosecond accuracy for timing of individual x-ray events [11].

The measured x-ray fluxes are compared with simulations using the Fokker-Planck code CQL3D [12], which solves for the bounce-averaged electron distribution $f(u, \theta, r)$ as a function of momentum per unit mass ($u = p/m$), pitch angle in velocity space (θ), and radius (r). The fully relativistic solution, needed for calculations using electron energies up to $\sim$100 keV is computed from the self-consistent evolution of test particles defined by Maxwellian distributions with the measured profiles of electron density (n_e), and electron and ion temperature ($T_{e,i}$). Impurity concentration, important for resistivity and bremsstrahlung modeling, is simulated by the inclusion of a single high Z impurity species. Current profiles and the mean-field 2D magnetic flux surfaces are supplied by equilibrium reconstruction [13].

The code determines the bounce-averaged electron distribution function, governed by the Fokker-Planck (FP) equation:

$$\frac{df}{dt} = \nabla_{\mathbf{u}} \cdot \Gamma_{\mathbf{u}} + R(f). \quad (1)$$

The FP operator $\nabla_{\mathbf{u}} \cdot \Gamma_{\mathbf{u}} = C(f) + E(f)$, where $C(f)$ is the Coulomb collision term and $E(f)$ is the electric field term. The radial diffusion operator $R(f)$ is composed of a diffusive part and an advective part:

$$R(f) = \frac{1}{r}\frac{\partial}{\partial r} r\left[D_\rho\left(\frac{v_{||}}{v_{th}}\right)^\alpha \frac{\partial}{\partial r} - V_r\right] f, \quad (2)$$

where D_ρ is the spatially varying radial diffusion coefficient for the bulk electrons, $v_{||}$ is the parallel electron velocity, $v_{\rm th}$ is the electron thermal velocity, and V_r is the pinch velocity, which is chosen to balance the diffusion losses automatically and preserve the input density profile. The overall electron particle diffusion is $D_r = D_\rho(v_{||}/v_{\rm th})^\alpha$. D_ρ governs the overall level of diffusion and the parameter α changes the velocity dependence of the diffusion: $\alpha = 1$ corresponds to a diffusion model consistent with stochastic magnetic transport; $\alpha = 0$ allows no energy dependence to the diffusion coefficient, suggestive of diffusion driven by electrostatic fluctuations. Solution for D_ρ and α is obtained by varying these quantities in $R(f)$ to match simultaneously the resistivity profile and HXR flux.

The resistivity profile most strongly constrains the bulk electron radial diffusion coefficient, represented by D_ρ. An initial guess for the parallel electric field [$E_{||} = (\mathbf{E} \cdot \mathbf{B})/|B|$] profile is given by the product of the measured parallel current density [$J_{||} = (\mathbf{J} \cdot \mathbf{B})/|B|$] [14] and the computed Spitzer resistivity (based on the input density, temperature, and impurity concentration profiles). This determines the operator term $E(f)$. An initial guess for D_ρ is specified. The CQL3D code then solves the Fokker-Planck equation for the electron distribution function which is then used to compute the resistivity directly, including neoclassical, radial transport, and fast electron effects. The computed $J_{||}$ is compared with the experimental value, giving a new estimate for the parallel electric field. This process is repeated iteratively until a self-consistent $E_{||}$ and $J_{||}$ are found. At this point, the resistivity profile is compared with the measured value from equilibrium reconstruction. The value of D_ρ is varied, and the code is reexecuted until a best match is found.

The HXR flux most strongly constrains the velocity dependence of the diffusion, represented by α. The computed line-integrated HXR flux is compared with the measured value, and α is varied and the code reexecuted until the best match is found. The modeling has been applied to both standard and improved-confinement plasmas.

Standard plasmas in MST are characterized by large-amplitude magnetic fluctuations, high Ohmic input power, and low HXR flux. The core magnetic fluctuation level is typically 1–2% of the equilibrium field strength, but increases transiently to $\sim$4% during sawtoothlike reconnection events [15]. The radial component of the fluctuations allows field lines to deviate from closed flux surfaces. This results in field lines which, it is believed, wander stochastically across the plasma. There is strong evidence linking magnetic fluctuations to transport, both from probe measurements of magnetic fluctuations [16] and from comparison of the bulk thermal conductivity with the theoretical expectation for stochastic magnetic transport [17]. This model of diffusion corresponds to $\alpha = 1$ in Eq. (2).

The measured profiles of temperature, density, and $J_{||}$ for a 400 kA standard plasma shown in Fig. 1 (dashed lines) were used for the modeling. Best fit to both the resistivity profile and the HXR flux is found for $D_\rho = 25\ \mathrm{m^2/s}$ and $\alpha = 1$, as shown in Fig. 2 (dashed lines). Thus, transport in standard plasmas is found to be consistent with stochastic magnetic field diffusion.

MHD calculations have shown that the addition of appropriate edge current using auxiliary current drive could reduce the tearing mode fluctuations and associated transport [18]. Recent MST experiments using an inductive technique called pulsed poloidal (or parallel) current drive (PPCD) have achieved this. There is a reduction in the tearing mode amplitudes, and the energy confinement time increases by an order of magnitude [3]. Simultaneously, the HXR flux due to emission from runaway electrons increases by at least 2 orders of magnitude and its fall-off with increasing energy slows.

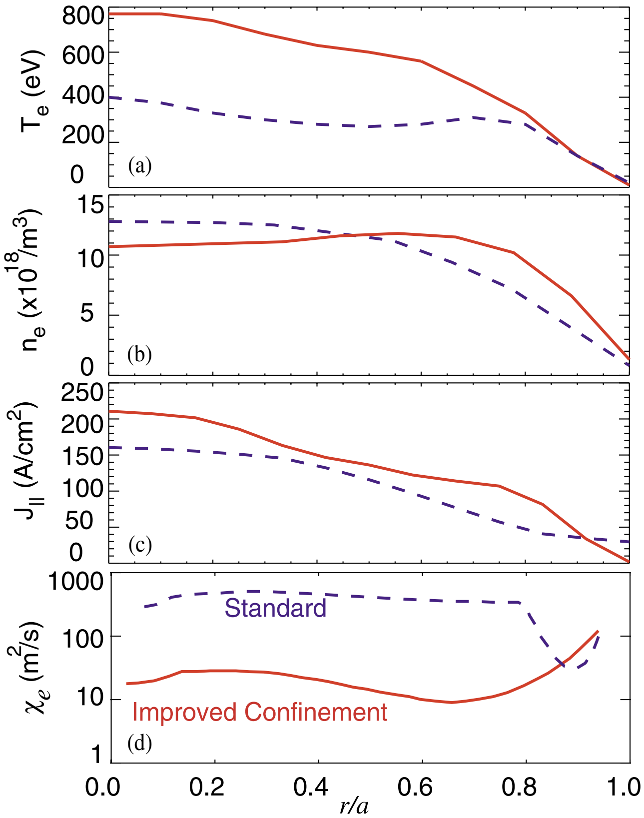

FIG. 1 (color online). Radial profiles of plasma parameters during standard discharges (dashed lines) and PPCD (solid lines), (a) the electron temperature, (b) the electron density, (c) the parallel current density and (d) the electron heat diffusivity.

Figure 3 shows the HXR emission from runaway electrons as the plasma enters PPCD induced improved-confinement period. The HXR flux is extremely low before the application of PPCD and the magnetic fluctuation amplitude ($\tilde{b}$) is 2–3%. At 8 ms PPCD is initiated; by $\sim$11 ms the additional current driven has begun to reduce the resistive tearing modes [Fig. 3(b)], and $\tilde{b}$ drops to $<$1% and a HXR signal emerges [Fig. 3(a)]. At $\sim$16 ms the flux saturates. By $\sim$20 ms the driven current profile control ends; the resistive tearing modes grow, and the HXR flux drops rapidly back to zero, as is expected with the return to stochastic magnetic dominated transport. Figure 1 also shows the measured electron and current density profiles during PPCD at 16.5 ms into a typical discharge. The discharges are chosen to have the same electron density ($n_e \cong 1.2 \times 10^{19}$ m^{-3}) as the standard plasma case. The core electron temperature during the PPCD discharge is $\sim$800 eV, approximately double the standard plasma value. The measured heat diffusivity χ_e is approximately an order of magnitude lower during PPCD plasmas compared with standard plasmas [17], as shown in Fig. 1(d).

Simple analysis of the emission spectrum suggests a change in the transport mechanism. During PPCD the measured particle confinement time is $\sim$5 ms [19]. Stochastic magnetic transport models imply smaller confinement time for higher energy electrons. Their velocity is $\gtrsim$10 times the bulk thermal velocity, so a confinement time of $<$0.5 ms is expected. Yet, for the measured electric field ($\sim$0.4 V/m), *collisionless* acceleration of an electron to 100 keV would require $\sim$3 ms (longer with collisions). This is similar to the bulk electron confinement time. In this time the electron travels $\approx$100 km. This suggests that stochastic magnetic transport, which adequately describes standard plasmas, is not a good model for PPCD plasmas. It should be noted that despite

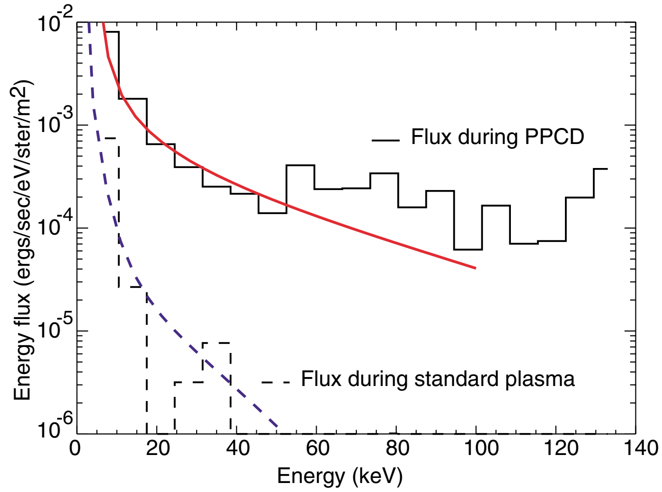

FIG. 2 (color online). Measured HXR flux for standard plasma (dashed histogram) is best fit (dashed curve) using a diffusion coefficient proportional to the parallel electron velocity ($\alpha = 1$). Measured HXR flux in improved confinement plasma (solid histogram) is best fit (solid curve) using diffusion coefficient which is velocity independent ($\alpha = 0$).

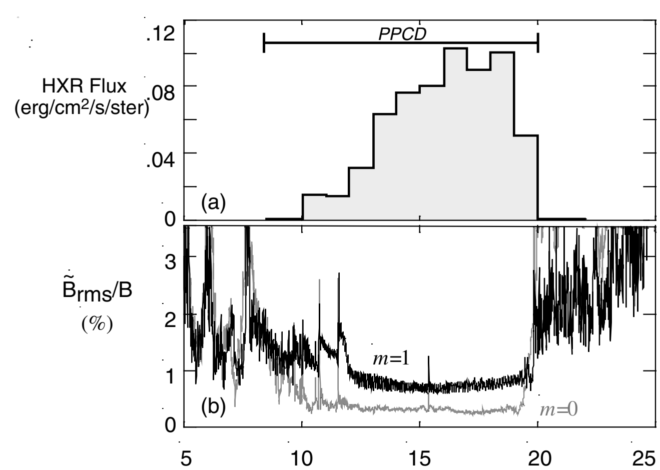

FIG. 3. The integrated HXR flux for energy beyond 20 keV (a) and the rms fluctuation amplitude as a percentage of the equilibrium field (b) versus time for a 400 kA improved confinement PPCD discharge. Modeling shows that this flux corresponds to a runaway electron population of $\sim$1–2%.

the large increase in peak electron energy to 100 keV, the gyroradius is still ~1.5 mm, smaller than the radial scale length of the magnetic fluctuations.

These heuristic estimates are consistent with the detailed Fokker-Planck modeling. The modeling finds the particle diffusion coefficient to be 3 m^2/s, an order of magnitude lower than that of the standard case. The measured HXR flux, which is orders of magnitude higher than for standard plasmas, is shown in Fig. 2. The diffusion coefficient model that best fits the HXR data is independent of energy ($\alpha = 0$). A diffusion coefficient proportional to the parallel electron velocity, as was used for standard plasmas, would yield a HXR flux which is orders of magnitude lower than that which is measured.

It has been determined recently that a radial diffusion coefficient which is constant as a function of velocity gives good agreement between bulk and tail transport for the electron cyclotron wave heated TCV tokamak [20]. Thus, it appears that the improved-confinement regime of the RFP is exhibiting behavior similar to the tokamak. Indeed, the confinement of the RFP is approaching that of a tokamak of similar size, shape, and plasma current, illustrated by comparison with the world tokamak database [21–23].

In summary, the strong enhancement of a hard-x-ray flux, caused by bremsstrahlung emission of suprathermal electrons during improved-confinement PPCD plasmas in MST, is evidence that global magnetic transport has been significantly reduced, perhaps leading to the formation of closed flux surfaces. Fokker-Planck modeling suggests that a transition away from stochastic magnetic transport has occurred, with the diffusion coefficient no longer proportional to, but independent of parallel electron velocity, similar to recent observations for a tokamak.

This work was supported by the U.S. Department of Energy. The authors wish to recognize the many contributions of the UW-Madison MST group, including collaborators from UCLA; David Brower and Weixing Ding and CEA Cadarache; Yves Peysson and Léna Delpech.

---

*Electronic address: roconnell@wisc.edu
†Current address: Princeton Plasma Physics Laboratory, Princeton, NJ, USA.
‡Department of Electrical Engineering, University of California at Los Angeles, Los Angeles, CA 90095-1594, USA.
Current address: Princeton Plasma Physics Laboratory, Princeton, NJ, USA.

[1] J.W. Connor, Plasma Phys. Controlled Fusion **35**, B293 (1993).
[2] A. B. Rechester and M. N. Rosenbluth, Phys. Rev. Lett. **40**, 38 (1978).
[3] B. E. Chapman *et al.*, Phys. Rev. Lett. **87**, 205001 (2001).
[4] B. E. Chapman *et al.*, Phys. Plasmas **9**, 2061 (2002).
[5] A. H. Boozer and R. B. White, Phys. Rev. Lett. **49** 786 (1982).
[6] B. Alper *et al.*, Plasma Phys. Controlled Fusion **30**, 843 (1988).
[7] Y. Yagi, T. Shimada, Y. Hirano, and K. Hattori, in *Proceedings of 17th EPS Conference on Controlled Fusion and Plasma Heating, Amsterdam, The Netherlands, 1990* (Max-Planck-Institut für Plasmaphysik, Garching bei München, 1991).
[8] J. C. Ingraham, R. F. Ellis, J. N. Downing, C. P. Munson, P. G. Weber, and G. A. Werden, Phys. Fluids B **2** 143 (1990).
[9] R. N. Dexter, D.W. Kerst, T.W. Lovell, S. C. Prager, and J. C. Sprott, Fusion Technol. **19**, 131 (1991).
[10] Y. Peysson and F. Imbeaux, Rev. Sci. Instrum. **70**, 3987 (1999).
[11] R. O'Connell, D. J. Den Hartog, C. B. Forest, and R.W. Harvey, Rev. Sci. Instrum. **74**, 2001 (2003).
[12] R.W. Harvey, in Summary of the IAEA Technical Committee Meeting on Advances in Simulation and Modeling of Thermonuclear Plasmas, Montreal, 1992; U.S. Department of Commerce, NTIS, Doc. No. DE93002962, 1992.
[13] J. Anderson, Ph.D. thesis, University of Wisconsin, 2002.
[14] D. L. Brower, W. X. Ding, S. D. Terry, J. K. Anderson, T. M. Biewer, B. E. Chapman, D. Craig, C. B. Forest, S. C. Prager, and J. S. Sarff, Phys. Rev. Lett. **88**, 185005 (2002).
[15] D. J. Den Hartog, J. T. Chapman, D. Craig, G. Fiksel, P.W. Fontana, S. C. Prager, and J. S. Sarff, Phys. Plasmas **6**, 1813 (1999).
[16] G. Fiksel, S. C. Prager, W. Shen, and M. R. Stoneking, Phys. Rev. Lett. **72**, 1028 (1994).
[17] T. M. Biewer, C. B. Forest, J. K. Anderson, J. S. Sarff, S. C. Prager, G. Fiksel, B. Hudson, S. D. Terry, W. X. Ding, and D. L. Brower, Phys. Rev. Lett. (to be published).
[18] C. Sovinec and S. Prager, Nucl. Fusion **39**, 777 (1999).
[19] N. E. Lanier, D. Craig, J. K. Anderson, T. M. Biewer, B. E. Chapman, D. J. Den Hartog, C. B. Forest, S. C. Prager, D. L. Brower, and Y. Jiang, Phys. Rev. Lett. **85**, 2120 (2000).
[20] R.W. Harvey, O. Sauter, R. Prater, and P. Nikkola, Phys. Rev. Lett. **88**, 205001 (2002).
[21] ITER Physics Expert Group on Confinement and Transport and Confinement Modelling, Nucl. Fusion **39**, 2175 (1999).
[22] J. S. Sarff *et al.*, in Proceedings of the 19th IAEA Fusion Energy Conference, Lyon, France, 2002.
[23] J. S. Sarff *et al.*, Nucl. Fusion (to be published).